Visual Abstract

# $Al_2O_3$ and $T_iO_2$ flux enabling activated tungsten inert gas welding of 304 austenitic stainless steel plates

H. S. Patil, D. C. Patel
*Mechanical Engineering Department, GIDC Degree Engineering College, Abrama, Navsari, Gujarat, India*
*hspatil28@gmail.com, pateldcp@gmail.com*

**ABSTRACT.** Gas tungsten arc welding (GTAW) is an important in manufacturing industries where it is significant to control the mechanical and metallurgical characteristics and its weld bead geometry. This research work has been committed to study the influence of oxide fluxes on welding of 4 mm thick 304 austenitic stainless steel plates. The $Al_2O_3$ and $TiO_2$ were used as an oxide flux in powder form and are mixed with the acetone. The prepared mixture is then applied on bead plate without any joint preparation and without filler wire addition. The Taguchi method with $L_9$ orthogonal array has been used to determine the optimal weld process parameters. The current work aims to explore the influence of weld parameters on weld bead geometry (i.e. weld bead width, penetration and angular distortion), and mechanical and metallurgical characteristics for 304 stainless steel welds. The oxide flux seems to narrow the arc and thereby the current density increases at the anode spot, that results in high weld depth.

**KEYWORDS.** ATIG; Oxide flux; 304 stainless steel; Weld morphology; Angular distortion; Mechanical characteristics.



**Citation:** Patil H. S., Patel D. C., $Al_2O_3$ and $TiO_2$ flux enabling activated tungsten inert gas welding of 304 austenitic stainless steel plates, Frattura ed Integrità Strutturale, 61 (2022) 59-68.

**Received:** 24.02.2022
**Accepted:** 29.03.2022
**Online first:** 14.04.2022
**Published:** 01.07.2022



## INTRODUCTION

GTAW (Gas tungsten arc welding) is the most commonly used process for joining the stainless steel components. It is usually suitable for thin sheets due to its easier applicability, flexibility, and better economy and normally used for welding hard-to-weld metals such as stainless steels, aluminium, magnesium, copper and copper, and titanium [1-3]. Austenitic stainless steels 304 are typically used in constructing the nuclear power plant because of their excellent combination of strength and ductility and high resistance to oxidation and corrosion. The main significant characteristics of the TIG process are its good mechanical properties and high quality metallurgical welds. However, the TIG welding process have a few limitations like low penetration depth, and beyond 3 mm work piece thickness it is necessary to perform edge preparation (chamfer) and addition of filler material by multi pass welding. Cast-to-cast compositional variation in the base metal being welded also affected the TIG welds [4, 5]. One of the most notable techniques for overcoming these limitations is the use of activating flux in the TIG welding process. Paton Electric Welding Institute first proposed the activated tungsten inert gas (ATIG) welding process in the 1960s, which increases penetration [6-7]. Activating flux is a suspension of inorganic material in a volatile medium. Activating flux is made by

combining powder ingredients such as chlorides, oxides, and fluorides with an ethanol solvent or acetone to create a paint-like constituent. A thin layer of activating flux was applied on to the surface of the work piece to be welded before weld operation [8-12]. Activated Tungsten Inert Gas (ATIG) welding significantly improves weld pool penetration and is typically accomplished by applying a thin layer of active flux composition on the surface of the metal substrate. For stainless steel material, ATIG improves over conventional GTAW by increasing joining thickness from 6 to 10 mm for single pass [13]. Furthermore, compared with conventional TIG welding, the refinement in microstructure and superior mechanical characteristics of the austenitic stainless steel weld joint have been also reported [14−15]. The activated flux may have two types of mechanisms, one based on the Marangoni convection effect, and the other based on weld arc behaviour. Heiple and Roper [16-17] and Heiple et al. [18] proposed surface active elements in the molten pool change the temperature coefficient of surface tension from negative to positive, thereby reversing the Marangoni convection direction from outward to inward. As the direction of the fluid flow in the molten pool becomes inward, the joint penetration increases dramatically. Lucas [19] and Howse [20] associated the greater penetration of activated TIG welding to a constriction of the arc. However, with respect to detailed components and proportions of the activated fluxes, very few literatures were reported, also due to limited data are available in literature about the action of weld arc and the mechanisms requires further investigation. Information on these processes is essential to determine the TIG penetration capability improvement function of the activated flux. As austenitic stainless steels have a high coefficient of thermal expansion and low thermal conductivity than carbon/alloy steel, it can induce a large amount of shrinkage and distortion after welding. Determining the effect of the activated flux on weld distortion is essential to improving the performance of the stainless steel activated TIG technique. Hence, in current work, 4 mm thick 304 stainless steel plates were welded by ATIG method without groove preparation in a single pass, wherein the activated fluxes are self-developed and mainly consist of oxides, including $TiO_2$, $Al_2O_3$. The investigation aimed to explore the ATIG welding of 304 stainless steel and to analyse the influence of oxide fluxes and weld factors on weld bead geometry (i.e. weld bead width, penetration and angular distortion), mechanical and metallurgical characteristics. Information extracted from the experiments conducted in this study can be useful for the application in various manufacturing industries.

## MATERIALS AND EXPERIMENTAL METHODS

The weight % chemical compositions and mechanical characteristics of austenitic stainless steel 304 listed in Tab.1 were used in experimental analysis. In present study the plates were cut into strips of 150 x 75 mm of 4 mm in thickness, which were roughly polished with 240 grit flexible abrasive papers of silicon carbide to remove surface impurities, and then cleaned with acetone. Prior to the TIG welding process, activated flux was prepared by mixing powder forms of $Al_2O_3$, $TiO_2$ with acetone and a thin layer less than 0.25 mm was brushed onto the surface of the weld to be welded. Fig.1 shows schematic illustrations of mixing and coating of flux for TIG welding process. To create bead on plate welds, autogenous TIG welding was performed on 304 stainless steels. A machine-mounted torch with standard 2% thorium tungsten electrode of 3.2 mm diameter and high purity argon (15L/min) were fixed in all welds. The tip configuration of the electrode was a blunt point with a $45^0$ include angle. Tab.2 lists the weld process factors used in current study.

| C | Cr | Ni | Mn | Si | P | S | Fe | Tensile Strength, MPa | Yield Strength, MPa | Poisson's Ratio | % Elongation |
|---|---|---|---|---|---|---|---|---|---|---|---|
| 0.06 | 18.67 | 8.53 | 1.89 | 0.42 | 0.032 | 0.06 | Bal. | 605 | 290 | 0.25 | 32 |

Table 1: Chemical compositions (wt. %) and mechanical properties of austenitic stainless steel 304.

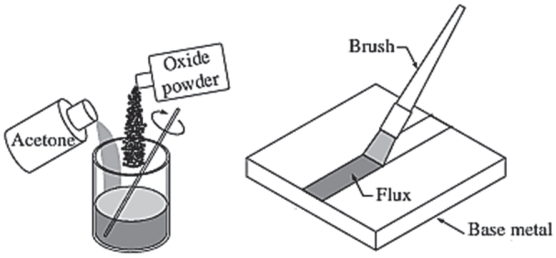


Figure 1: Schematic diagram of mixing and coating of flux for TIG welding.

| Weld Variables | Level-1 | Level-2 | Level-3 |
|---|---|---|---|
| Welding Current (A) | 180 | 200 | 220 |
| Welding Voltage (V) | 20 | 25 | 30 |
| Weld Gap (mm) | 0.5 | 0.75 | 1 |

Table 2: Welding process variables and experimental design levels of Taguchi method.

## RESULTS AND DISCUSSION

### *Influence of oxide fluxes on weld morphology*

In TIG welding process, molten metal flow takes place from center to the edges as the surface tension at the center of the weld pool is lower than that at the edges. These results in the more content of melt distributing near the edges of WFS (weld fusion zone) than that in the center i.e. less depth and more width of the weld pool. When fluxes other than stable oxides like $Al_2O_3$ are added, the Marangoni effect reverses, resulting in a greater increase in weld depth and a much smaller decrease in bead width. The TIG weld cross-sections with and without oxide fluxes for 4 mm thick stainless steel 304 plates are shown in Fig.2 It has been observed that in a A-TIG weld morphology, there is major variation in weld depth and bead width. With the use of $TiO_2$ oxide, the weld depth increases and the bead width decreases and have peanut shell type shape. With respect to conventional TIG welding, there is highest improvement in the penetration capability function with the use of $TiO_2$ i.e. up to 115%.

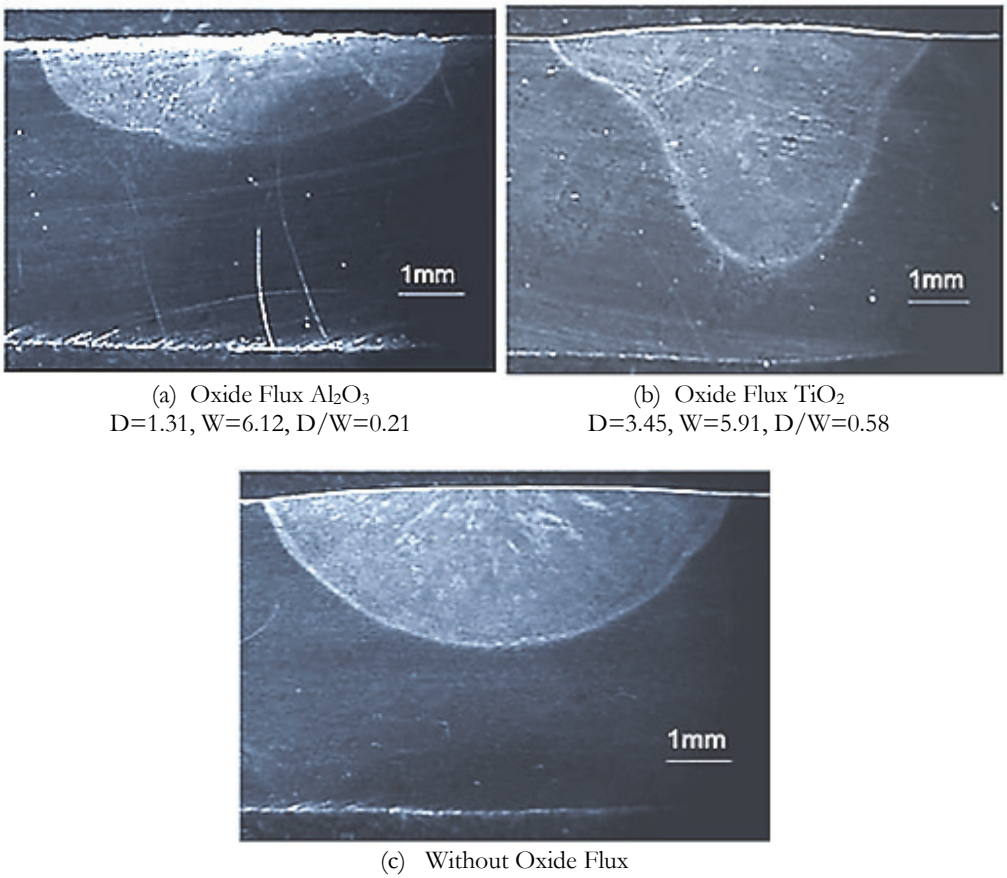


(a) Oxide Flux $Al_2O_3$
D=1.31, W=6.12, D/W=0.21

(b) Oxide Flux $TiO_2$
D=3.45, W=5.91, D/W=0.58

(c) Without Oxide Flux
D=2.11,W=7.79, D/W=0.27

Figure 2: Influence of oxide fluxes on weld morphology.

The weld depth to bead width ratio increased significantly with $TiO_2$ oxide TIG welding, as shown in Fig. 2. Previous studies have shown that the greater weld depth-bead width ratio and a narrower heat-affected zone are characterized by high energy density of the heat source and high energy concentration during the TIG welding process (21-22). Although ATIG penetration hasn't been proven by a common mechanism, it has commonly been observed in TIG welding that using activating flux can reduce the welding arc and therefore increase penetration (23-24). Activating fluxes seem to have a more profound effect on the welding arc characteristic than on the fluid flow direction (23, 25-27). Fig. 3 illustrates the central part of the welding arc clearly in a glowing zone occupying almost the entire length of the welding arc without flux and with $TiO_2$ composition. This zone is commonly considered the plasma column, which forms when the shielding gas is heated to ionize electrons and positively charged ions.

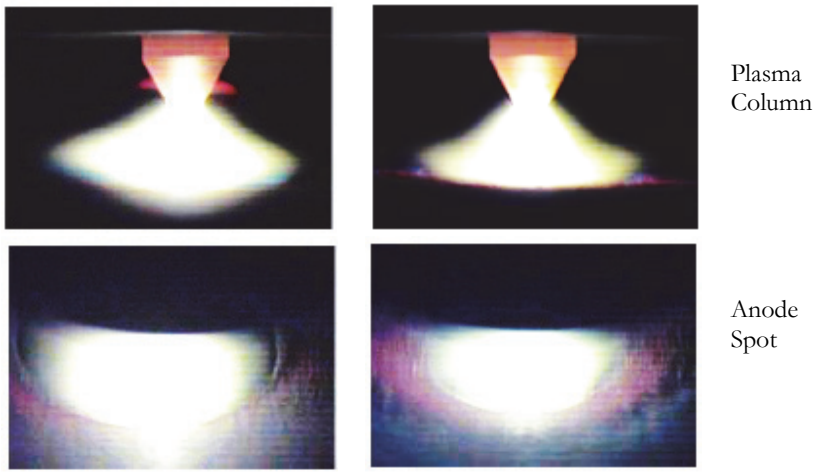


Figure 3: Arcing without flux and with $TiO_2$.

At the same current level, when the $TiO_2$-TIG welding arc is compared to a conventional TIG welding arc, the diameter of plasma column is narrowed. Due to a narrowed plasma column, the current density in the arc root increases, resulting in a greater arc in the A-TIG penetration than conventional TIG. Weld morphology can also be affected by anode spots.
Since the conductivity of the flux is much lower than that of the metal vapor and the melting point and boiling point of the flux are higher than that of the weld metal, metal evaporation occurs only in the central region of the weld arc where the temperature exceeds the dissociation temperature of flux compounds, thereby reducing the conductive region of the anode spot. It can also be seen that the anode spot is reduced with TIG weld pools with $TiO_2$ in comparison to conventional TIG welds at the same current level.
According to the present findings, the plasma column and anode spot have major impacts in determining ATIG weld morphology. When ATIG welding is employed, the plasma column is constricting physically, the anode spot is reduced, and the heat source energy, and the electromagnetic force emitted from the weld pool are increased, producing relatively narrow and deep welds compared to conventional TIG welding. Further research is needed to understand the mechanism, but current research shows the potential impact of of specific flux on ATIG penetration. The $Al_2O_3$ deteriorated penetration and excessive slag compared with conventional TIG for 304 stainless steel welds.
This can be seen in Fig. 4 where the TIG welding process with active flux, which contains $Al_2O_3$ powder, seems unable to reduce the anode spot and constrict the plasma column, leading to a relatively wide and shallow morphology of the weld in comparison to conventional TIG welding. The result can be attributed to the aluminium oxide particles in the weld pool during TIG welding with $Al_2O_3$ powder, as shown in Fig.4.
As TIG welding with $Al_2O_3$ produces fluid flow outwards from the center of the weld pool, the particle-free band will be formed along the edge of the weld pool, resulting in an arc wander.

*Influence of oxide flux on angular distortion*

During the welding process, the weld metal and the adjacent base material expand and contract, causing distortion of the weld. Because of the non-uniform shrinkage caused by uneven heating throughout the thickness of the joint plate during welding, an angular distortion appears in the weldment.

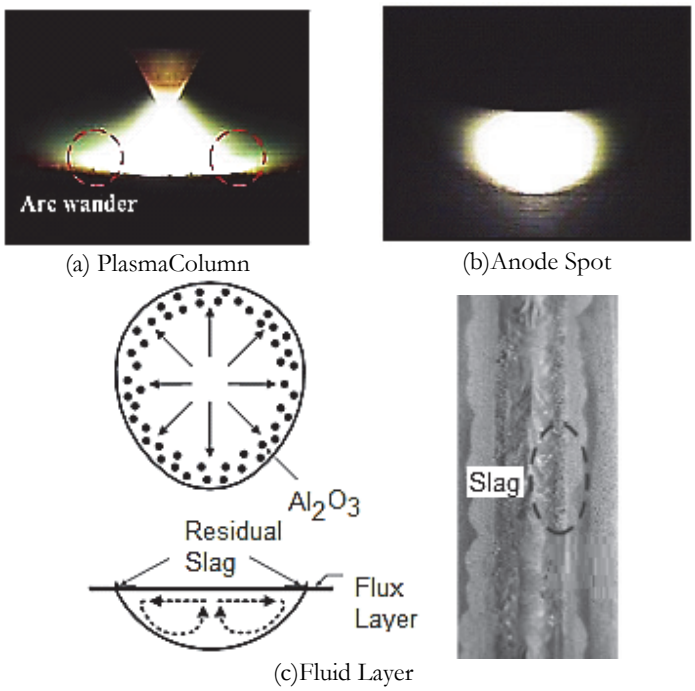


Figure 4: Effect of $Al_2O_3$ flux on welding arc and fluid flow.

Fig. 5 illustrates the influence of weld depth to plate thickness ratio on the angular distortion in stainless steel 304 with and without flux. It has clearly been shown that activated TIG welding results in a reduction in angular distortion of the weldment. In TIG welding with $Al_2O_3$ flux, the weld depth is not greater than half the thickness of the plate. When the weld depth is shallow in comparison to the thickness of the plate, the angular distortion of the weldment decreases; however, as the ratio of weld depth to plate thickness increases, the angular distortion of the weldment without flux increases until a critical point is reached (weld depth to plate thickness ratio is equivalent to 0.5).However, when weld depth becomes greater than 50% of the thickness of the plate, angular distortion of the weldment decreases with $TiO_2$. With activated TIG welding, we can experience a high degree of penetration into the joint and a high depth-width ratio, which indicates a high degree of energy concentration.

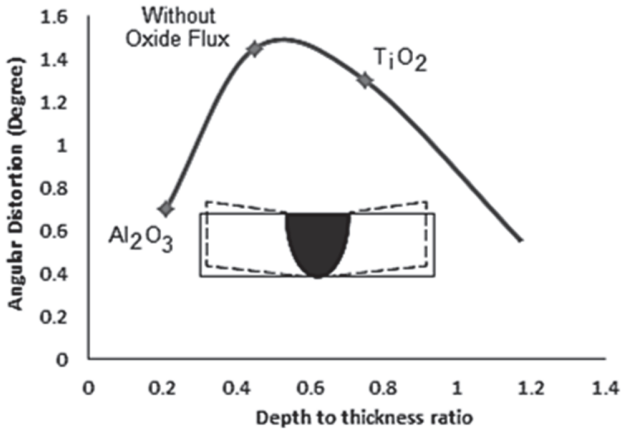


Figure 5: Effect of weld depth to plate thickness ratio on angular distortion.

Due to the reduced quantity of heat source, the base material is not overheated, and thermal stresses and incompatible strains can be reduced due to our reduced heat source. This results in reduced angular distortions when welding stainless steel 304.

Therefore, this result in a reduction in supplied heat source, which reduces the likelihood of overheating the base material and reduces the incidence of thermal stress and incompatible strain due to shrinkage in thickness and, therefore, can result in a reduction in 304stainless steel weldment angular distortions.

*Influence of oxide fluxes on mechanical characteristics*

Tensile test was carried out in 400 KN capacity mechanical controlled universal testing machine to determine the mechanical properties of the welded specimens. The test specimens used for tensile testing were cut from welded samples using water jet machine. The dimension of test specimen as per ASTM-E8 has been represented by Fig.6. The experimental results for mechanical characteristics of TIG weldments with and without activating fluxes are shown in Fig.7.

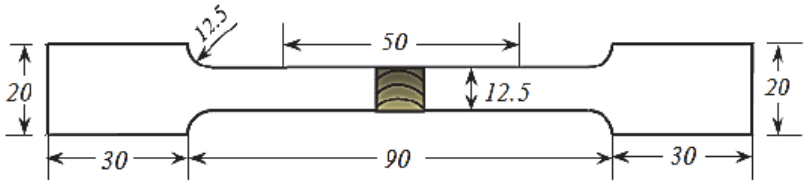


Figure 6: Tensile test specimens for welded samples (Dimensions are in mm).

It is obvious that the weldment produced by TIG welding with $TiO_2$ and $Al_2O_3$ has better mechanical qualities, such as ultimate tensile strength than the TIG weldment produced without the activating flux. At all arc voltages, raising the welding current from 180 to 220A will affect and enhance the tensile strength, as shown in Fig.7.

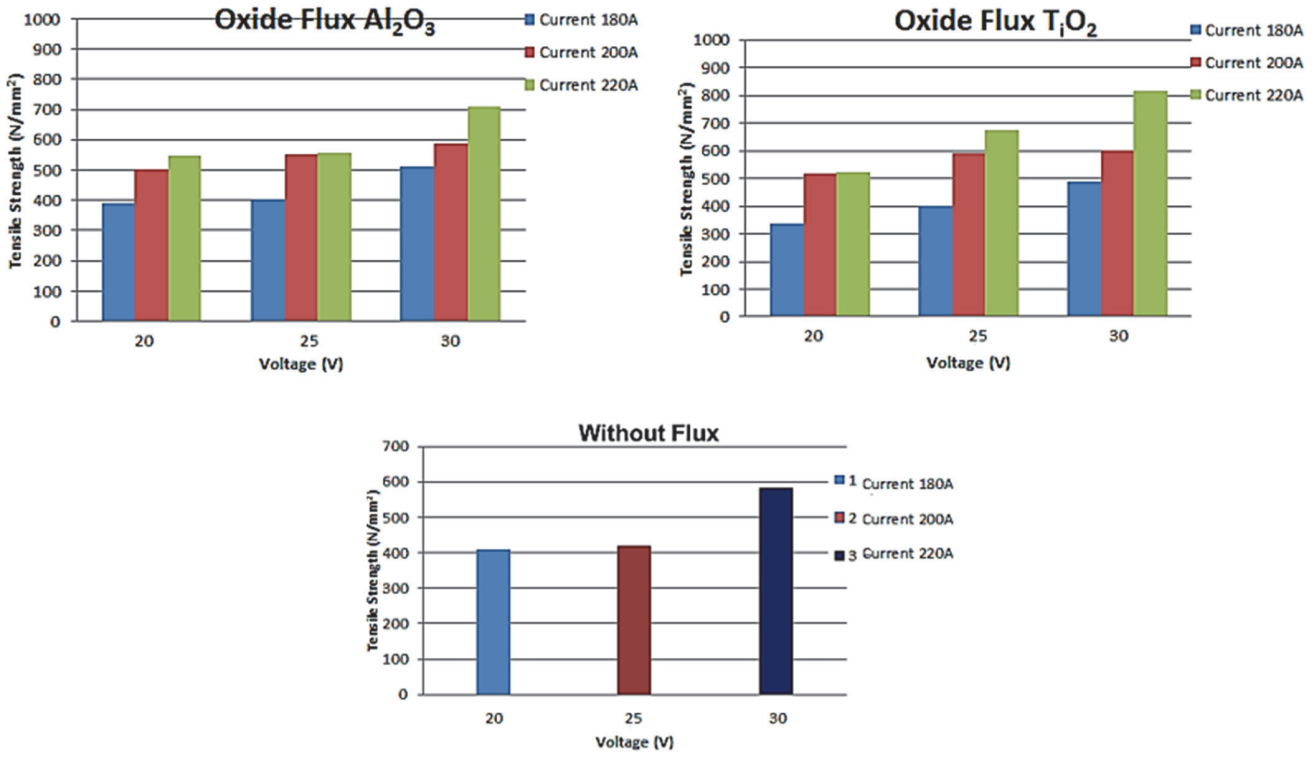


Figure 7: Mechanical properties of TIG welds.

Micro-indentation hardness test as per ASTM E-384:2006 has been used to measure the Vickers hardness of welded joints. The Vickers micro-hardness indenter is made of diamond in the form of a square-base pyramid. The test load applied was 100gm and the dwell time was 15 seconds. The indentations were made at midsection of the thickness of the plates across the joint. The experimental results for the hardness of the TIG welds with and without flux are shown in Fig.8. The findings revealed that the oxide flux had no discernible effect on the hardness of stainless steel weld metal. The crystal structure of austenite is cubic face-centered (FCC). The crystal structure of delta-ferrite is body-centered cubic

(BCC). The mechanical strength of the BCC structure is greater than that of the FCC structure. The delta-ferrite content in the weld metals is enhanced when TIG welding with or without flux is employed, which has a good effect on enhancing the hardness of stainless steel welds.

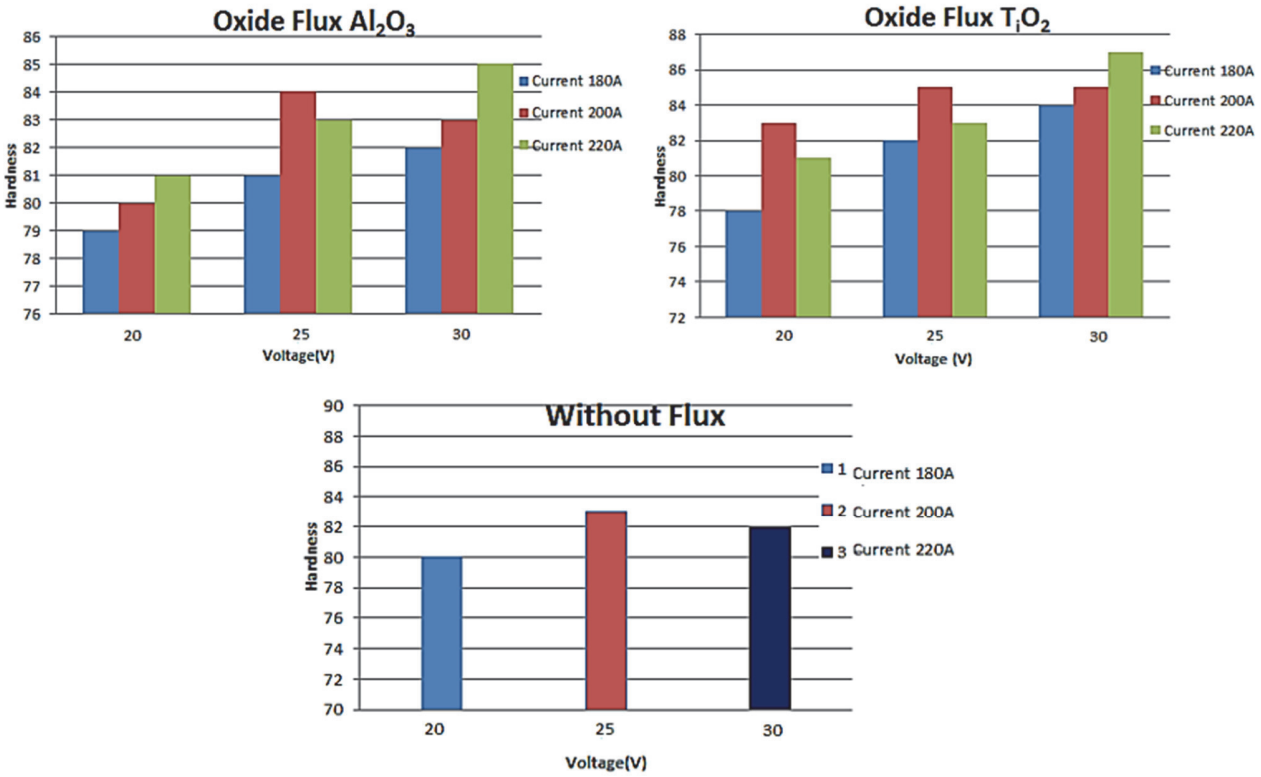


Figure 8: Hardness of TIG welds.

*Radiography analysis of ATIG weldments*

Weld samples were subjected to X-Ray radiographic inspection utilising a Radiographic unit in accordance with ASME section-VIII Div-I radiography standard techniques. The radioactive sources employed in the radiography test were 25Ci and Iridium Ir192. The RT technique used was SWSI, with a sensitivity of 2% and a development time of 5 minutes. The film utilised was Agfa D-4, and the radiographs revealed several flaws in the welds. In both the oxides $Al_2O_3$ and $TiO_2$, radiography investigation revealed a lack of penetration and insufficient fusion in TIG welded joints, as illustrated in Fig.9.

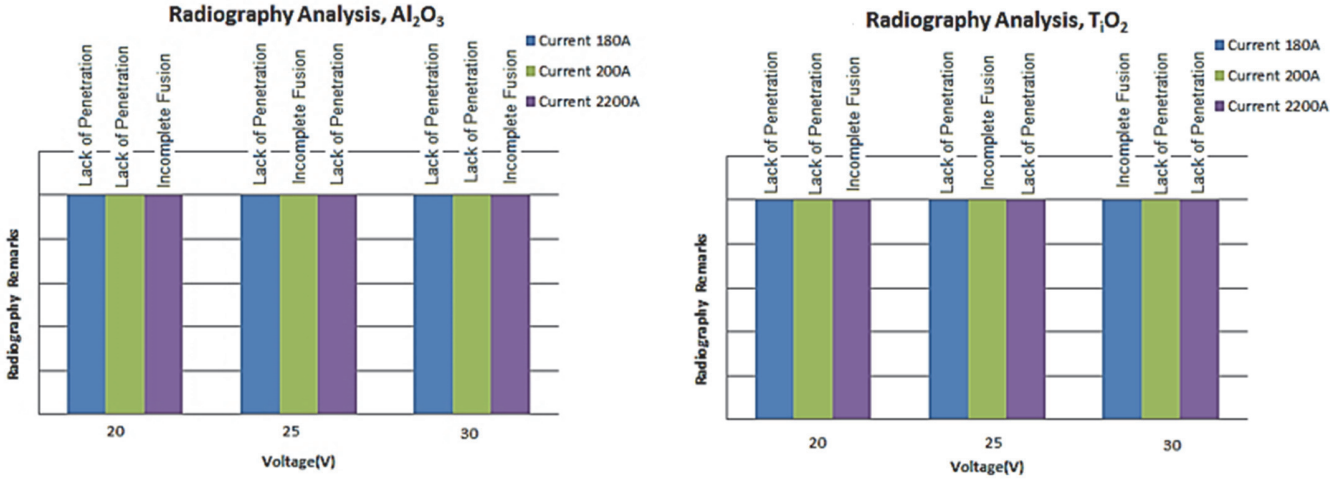


Figure 9: Radiography of TIG weld joints.

*Influence of flux on microstructures and delta-ferrite content*

The samples for optical microscopy were polished using grit silicon carbide paper. Etching procedures were used to expose the underlying microstructural features. Solutions used for etching titanium include a fresh Keller etchant with composition 5ml $HNO_3$, 3ml HCL, 2ml HF and 190ml distilled water. The polished metallographic mount was etched in the solution from 40 to 50 seconds to reveal the microstructural features. The fracture surfaces were analysed using scanning electron microscopy. Fig.10 depicts the microstructure of 304 stainless steel weld metal generated with and without flux, as well as the observed delta-ferrite content. The ferrite number was determined using a calibrating magnetic instrument. In this, stainless steel TIG welds produced without flux, the delta-ferrite content from its initial value of 1.7 FN is increased to 6.8 FN. This is because most of the weld metal of austenitic stainless steel solidified as delta-ferrite phase. During the welding process, the cooling rate of the weld metal was so fast that the phase transformation from delta ferrite to austenite was not completed. As a result, more delta ferrite remains in the weld metal after solidification. On the other hand, when the oxide flux was used, the delta ferrite content of the activated TIG weld metal increased slightly to 7.3 to 7.9 FN. The heat input during TIG welding with and without flux is related to this result. The weld current was kept constant, and it was discovered that when the activated TIG process was used, the arc voltage increased. Since the calculated heat input is proportional to the measured arc voltage, the applied activation flux has the positive effect of increasing the length of the heat input unit of the weld. This high heat input raises the peak temperature of the weld seam, which can result in the formation of more delta ferrite in the activated TIG weld metal. In all cases, the austenite matrix microstructure and vermicular delta ferrite morphology typical of this material class were found. However, there was no significant difference in the microstructure between conventional TIG weld metal and activated TIG weld metal.

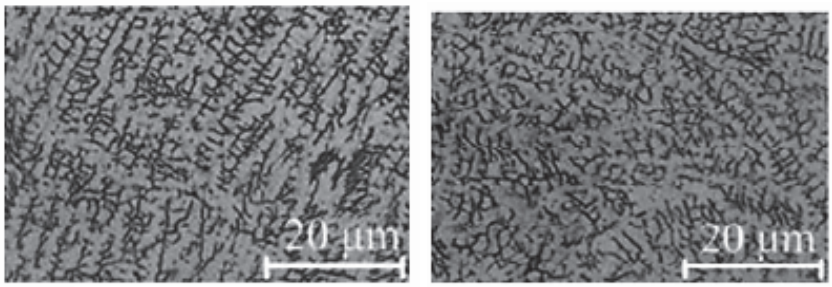


(a)Without Oxide Flux (b)With Oxide Flux $TiO_2$

(c)With Oxide Flux $Al_2O_3$

Figure 10: Microstructure and measured delta-ferrite content in 304 stainless steel weld.

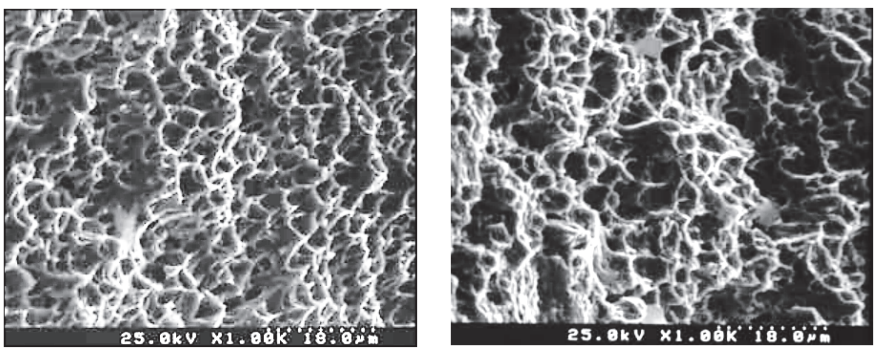


(a) With Oxide Flux $TiO_2$ (b) Without Oxide Flux

Figure 11: SEM images of fracture surface.

Fracture can be described as a single body divided into pieces by the applied stress. For engineering materials, there are only two types of fracture: ductility and brittleness. The fracture mode of TIG welding with oxide flux $TiO_2$ and no flux is ductile dimple fracture mode as shown in Fig.11.

## CONCLUSIONS

This research paper conducted detailed experiments to systematically investigate the influence of oxide fluxes $Al_2O_3$ and $TiO_2$ on weld morphology, angular distortion, delta-ferrite content, tensile strength and hardness when using the TIG process to weld 4mm thick 304 stainless steel plates on weld different parameters. The experimental results and conclusions are summarized as follows:

**a.** The use of $TiO_2$ resulted in significant increases in weld depth and decreases in bead width, as well as the greatest improvement function in penetration, whereas the use of $Al_2O_3$ resulted in deterioration in penetration and excessive slag when compared to the conventional TIG welding for a 304 stainless steel.

**b.** When using ATIG welding, physically constricting the plasma column and reducing the anode spot, tends to increase the energy density of the heat source and electromagnetic force of the weld pool, resulting in a relatively narrow and deep weld morphology compared with the conventional TIG welding**.**

**c.** Activated TIG welding can increase joint penetration and ratio of weld depth to width, decreasing the angular distortion of weldment significantly.

**d.** Better mechanical characteristics are retained by ATIG weldment.

**e.** A-TIG welding can increase the retained delta-ferrite content of stainless steel welds.

**f.** The optimum set parameters for oxide fluxes $TiO_2$ and $Al_2O_3$ are 180A, 20V, 0.75 mm and 220A, 30V, 0.75 mm respectively giving better weld characteristics.

## CONFLICT OF INTEREST

The authors declare that there is no conflict of interests regarding the publication of this paper.

## NOMENCLATURE/SYMBOLS

GTAW- Gas tungsten arc welding
ATIG- Activated Tungsten Inert Gas
BCC- Body Centered Cubic
FCC- Cubic Face Centered
FN-Ferrite Number
SWSI -Single Wall Single Image
D-Weld depth (mm)
W-Bead width (mm)

## REFERENCES

[1] Cary, H. B. (1989). Modern Welding Technology, Prentice Hall, Englewood Cliffs, New Jersey.
[2] Olson, D. L., Siewart, T. A., Liu, S. and Edwards, G. R. (1998). ASM Metals Handbook Vol. 6: Welding, Brazing, and Soldering, 10th Edition, ASM International.
[3] Kou, S. (2003).Welding Metallurgy, Libre Digital, Wiley, 2th ed. Wiley India
[4] Huang, H. Y., Shyu, S., Tseng, K-H. and Chou, C. P. (2005). Evaluation of TIG flux welding on the characteristics of stainless steel, Science and Technology of Welding and Joining, 10(5), pp. 566–573. DOI 10.1179/174329305X48329

[5] Shyu, S., Huang, H. Y., Tseng, K-H. and Chou, C. P. (2008). Study of the performance of stainless steel A-TIG welds, Journal of Materials Engineering and Performance, 17(2), pp. 197–201. DOI: 10.1007/s11665-007-9139-7
[6] Hdhibi, A. K., Touileb, R. and Djoudjou. (2018). Effect of Single Oxide Fluxes on Morphology and Mechanical Properties of ATIG on 316 L Austenitic Stainless Steel Welds, 8(3), pp. 3064-3072. DOI: 0.48084/etasr.2097
[7] Makara, A. M., Kushnirenko, B. N. and Zamkov, V. N. (1968). High-tensile martensitic steels welded by argon tungsten arc process using flux. Automatic Welding, 7, pp. 78-79.
[8] Huang, H. Y., Shyu, S., Tseng, K-H. and Chou, C. P. (2006). Effects of the process parameters on austenitic stainless steel by TIG-flux welding. Journal of Material Science Technology; 22(3) pp. 367-374. DOI: https://www.jmst.org/EN/Y2006/V22/I03/367
[9] Lu, S. P., Li, D. Z., Fujii, H. and Nogi, K. (2007). Time dependant weld shape in $AreO_2$ shielded stationary GTA welding, Journal Material Science Tech, 23(5), pp. 650-654. DOI://www.jmst.org/EN/Y2007/V23/I05/650
[10] Tseng, K-H. and Hsu, C. Y. (2011). Performance of activated TIG process in austenitic stainless steel welds. Journal Material Processing Technology; 211(3), pp. 503-512. DOI:10.1016/j.jmatprotec.2010.11.003
[11] Chern, T. S., Tseng, K-H. and Tsai, H. L. (2011). Study of the characteristics of duplex stainless steel activated tungsten inert gas welds. Material Design, 32(1), pp. 255-263. DOI: 10.1016/j.matdes.2010.05.056
[12] Gurevich, S. M., Zamkov, V. N. and Kushnirenko, N. A. (1965). Improving the penetration of titanium alloys welded by argon tungsten arc process, Avtomaticheskaya Svarka, 9, pp. 1-4.
[13] Leconte, S., Paillard, P., Chapelle, P., Henrion, G. and Saindrenan, J. (2006). Effect of oxide fluxes on activation mechanisms of tungsten inert gas process, Science and Technology of Welding and Joining; 11(4), pp.389-397.
[14] Rodrigues, A., Loureiro, A. and Batista, A. (2005). Proceeding IIW International Conference on Benefits of New Methods and Trends in Welding to Economy: Productivity and Quality, 58th Annual Assembly and International Conference of the IIW. Prague, pp. 415–425.
[15] Palanichamy, P., Vasudevan, M. and Jayakumar, T. (2009). Measurement of residual stresses in austenitic stainless steel welding joints using ultrasonic technology Journal of Science Technology Weld Joining, 14(2), pp. 66–171.
[16] Heiple, C. R. and Roper, J. R. (1981). Effect of selenium on GTAW fusion zone geometry, Welding Journal, 60 (8), pp.143–145
[17] Heiple, C. R. and Roper, J. R. (1982). Mechanism for minor element effect on GTA fusion zone geometry, Welding Journal, 61 (4), pp. 97–102
[18] Heiple, C. R., Roper, J. R., Stagner, R. T. and Aden, R. J. (1983). Surface active element effects on the shape of GTA. Laser and electron beam welds. Welding Journal. 62 (3), pp.72–77.
[19] Lucas, W. and Howse, D. (1996). Activating flux–increasing the performance and productivity of the TIG and plasma processes. Weld. Met. Fab. 64 (1), pp.11–17.
[20] Howse, D. S. and Lucas, W. (2000). Investigation into arc constriction by active fluxes for tungsten inert gas welding. Sci. Technol. Weld. Join. 5 (3), pp.189–193.
[21] Tseng, K-H. and Chou, C.P. (2001). Effect of Pulsed Gas Tungsten Arc Welding on Angular Distortion in Austenitic Stainless Steel Weldments, Science and Technology of Welding and Joining, 6(3), pp. 149–153. DOI: 10.1179/136217101101538686
[22] Tseng, K-H. and Chou, C.P. (2002). The Effect of Pulsed GTA Welding on the Residual Stress of a Stainless Steel Weldment, J. Mater. Process. Technol., 123, pp. 346–353. DOI:10.1016/S0924-0136(02)00004-3
[23] Huang, H. Y., Shyu, S., Tseng, K-H. and Chou, C. P. (2006). Effects of the Process Parameters on Austenitic Stainless Steel by TIG-flux Welding, Journal of Material Science Technology, 22(3), pp. 367–373. DOI: https://www.jmst.org/EN/Y2006/V22/I03/367
[24] Tanaka, M., Shimizu, T., Terasaki, H., Ushio, M., Koshi-ishi, F. and Yang, C. L. (2000). Effects of Activating Flux on Arc Phenomena in Gas Tungsten Arc Welding, Science Technology, Welding Joining, 2000, 5(6), pp. 397–402
[25] Huang, H. Y., Shyu, S., Tseng, K-H. and Chou, C. P. (2005). Evaluation of TIG-Flux Welding on the Characteristics of Stainless Steel, Science Technology, Welding Joining, 10(5), pp. 566–573
[26] Huang, H. Y., Shyu, S., Tseng, K-H. and Chou, C. P. (2005). Effect of A-TIG Welding on the Morphology of Stainless Steel Welds, Proceedings of 7th International Conference on Trends in Welding Research, ASM International.
[27] Sathiya, P. S., Aravinda, P. M., Ajith, B. and Arivazhagan, A. (2010).Microstructural Characteristics on Bead on Plate Welding of AISI 904 L Super Austenitic Stainless Steel Using Gas Metal Arc Welding Process, Engineering, Science and Technology, 2(6), pp. 189-199. DOI: 10.4314/ijest.v2i6.63710.